SLAC–PUB–10117
August 2002

Overview of NLC/JLC Collaboration *

K. Takata
KEK, Oho, Tsukuba-shi 305-0801, JAPAN

On behalf of the NLC Group
Stanford Linear Accelerator Center, Stanford, California 94309, USA

And the JLC Group
KEK, Oho, Tsukuba-shi 305-0801, JAPAN

Presented at LINAC 2002
Gyeongju, Korea
August 19 – 23, 2002

* Work supported by Department of Energy contract DE–AC03–76SF00515.

OVERVIEW OF NLC/JLC COLLABORATION

K. Takata*
KEK, Oho, Tsukuba-shi 305-0801, JAPAN

Abstract

The NLC/JLC collaboration focuses its major effort on X-band linac technology which is the main part of a 1 TeV electron-positron linear collider.

1 INTRODUCTION

Both SLAC and KEK have pursued R&D for a TeV linear collider over 15 years with the acronyms NLC (Next Linear Collider) and JLC (Japan Linear Collider). The two teams assumed X-band (11.424 GHz) warm linac technology for the main linac, although R&D for technology at C-band (5.712 GHz) has also been optionally undertaken at KEK.

The collaboration between SLAC and KEK is focused on the X-band linac technology and low-emittance beam generation study [1] at the ATF (Accelerator Test Facility) damping ring of KEK. In this collaborative framework, however, many other laboratories have also contributed: BINP (Protvino, Russia), Postech (Korea), IHEP and Tsinghua University (Beijing), LLNL, LBNL and recently FNAL (USA), and several universities worldwide.

Since 1998, 8 meetings have been held for the International Study Group (ISG), through which NLC and JLC are getting much closer in the design features and R&D directions.

The report below summarizes is the recent R&D status on X-band accelerating structures and RF power source together with some interesting results of the most-up-to-date beam monitors developed at the ATF damping ring.

2 NLC/JLC CONFIGURATION

Figure 1 shows the general layout of NLC/JLC accelerator complex. NLC and JLC take essentially the same geometrical configuration except for a small difference at present with respect to the crossing angle at the interaction point: NLC assumes 20 mrad, whereas JLC 7 mrad.

The two injectors for the main linacs are identical for electron and positron beams except for the additional linac to produce positrons. Each comprises a 1.98 GeV damping ring with an S-Band injection linac of the same energy and a two-stage bunch compressor system. One operation cycle produces a train of 192 electron/positron bunches with a bunch-to-bunch spacing of 1.4 ns and 7.5×10^9 particles/bunch. The repetition rate of the cycle is assumed to be 120 Hz if the site is built in regions where the AC line is operated at 60 Hz, and 150 Hz for $E_{CM} = 500$ GeV and 100 Hz for $E_{CM} = 1.0$ TeV if built in 50 Hz regions. The overall parameters are summarized in Table 1.

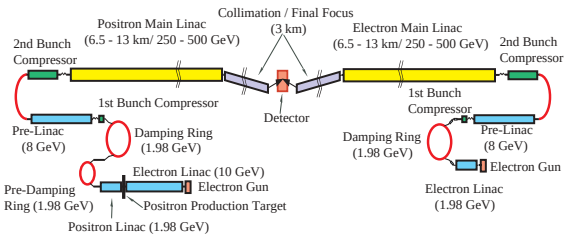

Figure 1: Simplified diagram of NLC/JLC configuration

Table 1: Overall Parameters

Center of mass energy (GeV)	500	1000
Linac RF frequency (GHz)	11.424	
Luminosity ($10^{33}\mathrm{cm}^{-2}\mathrm{s}^{-1}$)	25(20)*	25 (30)
Linac rep. rate (Hz)	150 (120)	100 (120)
# of particles/ bunch at IP	7.5×10^9	
# of bunches/ pulse	192	
Bunch separation (nsec)	1.4	
Proposed site length (km)	32	
Total two-linac length (km)	12.6	25.8
Total site AC power (MW)	215 (185)	280 (320)

* Numbers in ( ) for 60 Hz AC, otherwise for 50 Hz.

3 X-BAND MAIN LINACS

Either of the two main linacs accelerates 8 GeV beams delivered from the injection system to $E_{CM}/2$. The JLC linac optics is a simple repetition of a FODO lattice with a length of 2×6.534 m. The NLC optics is almost the same except for slightly longer unit lengths at downstream parts because the Q magnet length is made longer there. The 6.534 m linac unit has a 0.534 m section for a Q magnet and a cavity-type beam position monitor followed by a 6.000 m section where 6 accelerating structures are placed with a period of 1.0 m. The Q magnet has an iron pole length of 260 mm. At the present design stage the RF length of an accelerating structure is assumed to be 0.90 m or $\approx 34\ \lambda$. The total number of accelerator units is 1872 for $E_{CM} = 500$ GeV and 3744 for $E_{CM} = 1.0$ TeV.

The loaded and unloaded gradients in a structure are assumed to be 54.7 MV/m and 70 MV/m, respectively, which

*On behalf of NLC Group (SLAC, Stanford, CA 94309, USA) and JLC Group (KEK, Oho, Tsukuba-shi 305-0801, JAPAN)

are by an input power of 85 MW per structure. The filling time of a structure is 120 ns with the bunch train length being 267 ns. Hence the input pulse length is set as 400 ns with rise and fall times of a few ns.

RF power distribution is based on the delay-line-distribution system (DLDS). The details for this case are as follows. JLC uses 3744 klystrons for $E_{CM} = 500$ GeV and 7488 klystrons for $E_{CM} = 1.0$ TeV with 1.6 μs, 75 MW output pulses. NLC, however, assumes a pulse width of 3.2 μs with the same peak power and hence the numbers of klystrons are halved.

A group of 8 klystrons form an RF unit. The RF phase of every 400 ns section of output pulses of each tube is coded for 0 or π. The code sequence, different from one klystron to another, is so chosen that the outputs of the 8 klystrons are combined and then sliced into 400 ns, 600 MW pulses. They are sent through long waveguides and tapped off at 4 linac units for JLC and 8 units for NLC which are placed with a separation of 59.105 m. At each unit, the tapped-off power is divided into six pulses of one-sixth peak power for 6 accelerating structures which are comprised in the unit.

Table 2: Typical Parameters for the Main Linacs

Center of mass energy (GeV)	500	1000
Structure length (cm)	90	
RF power/ structure (MW)	85	
RF pulse length/ structure (ns)	400	
Unloaded gradient (MV/m)	70	
Loaded gradient (MV/m)	54.7	
# of structures/linac unit	6	
Length of linac unit (m)	6.534	
# of linac units	1872	3744
# of structures	11232	22464
Klystron peak power (MW)	75	
Klystron pulse length (μs)	$1.6(3.2)^*$	
# of JLC klystrons	3744	7488
# of NLC klystrons	1872	3744

* Number in ( ) for NLC.

4 ACCELERATING STRUCTURE

The structure study has progressed under close collaboration between the NLC and JLC teams. Electrical design, wake field measurements and high gradient test have been carried out by the NLC team, while fabrication study (precise machining with diamond turning, diffusion bonding etc.) by the JLC team.

4.1 Basic RF Features

Accelerating structures considered for the NLC/JLC are conventional traveling wave (TW) ones with the cell dimensions similar to one-fourth of those of S-band linacs. The phase shift per cell was at first $2\pi/3$, but a preference at the present design is $5\pi/6$ because of the reasons discussed in Subsection 4.2. The accelerating gradient is kept roughly constant over a structure. But great care should be taken for reduction of the dipole wakes and reliability at high gradient operation [2].

There are two issues regarding the dipole wakes. First, while a smaller aperture radius a may make a larger accelerating shunt impedance, the short range dipole wakes scale $\sim a^{-3.8}$. In fact simulations show a/λ should be 0.18 or larger. In this connection, structures with rounded cell profiles have also been studied besides conventional flat disk structures. Secondly, in order to cope with long range wakes, dominant dipole modes are damped and detuned cell by cell.

For the damping, short radial slots at every 90° are cut on the peripheral part of each disk. The slots are coupled with 4 damping manifolds (small circular waveguide) running through the whole length of the structure. The detuning is realized by modifying the cell profile dimensions cell by cell. The resultant density profile of the first dipole mode has a gaussian-like spectrum.

The electrical design considerations described above are realized as two types of structures: damped-detuned structures (DDS) and round-profile DDS (RDDS). Their details are given in Ref. [3]. Fabrication of copper disks with required dimensional accuracies, precise stacking and diffusion bonding of them are now well established technologies [4]. Good agreements with simulation have been obtained in a beam test at ASSET of SLAC.

Figure 2 shows an RDDS with its unit cell. Main updated parameters of a standard structure are summarized in Table 3.

Table 3: Updated Parameters for Accelerating Structure

Length		90	cm
Phase advance/ cell		150	deg
Iris radius	a/λ	$0.210 \rightarrow 0.148$	
Group velocity	v_g/c	$5.1 \rightarrow 1.1$	%
Filling time	T_f	120	ns
Attenuation parameter	τ	0.510	
Unloaded Q	Q	9055 $\rightarrow$ 8093	
Shunt impedance	r	81.2	MΩ

4.2 High Gradient Tests (HiGT)

Since basic RF design for both the accelerating mode and deflecting modes was almost completed, the most concern in these two or three years has been the RF breakdowns at high gradient operation. Through the series of tests it became clear that the dominant factors to achieve better high-gradient results were low group velocities, low-field/low-impedance couplers, and cell cleaning methods before test (particularly the chemical etching depth and baking). To date, over 10 TW structures underwent HiGT

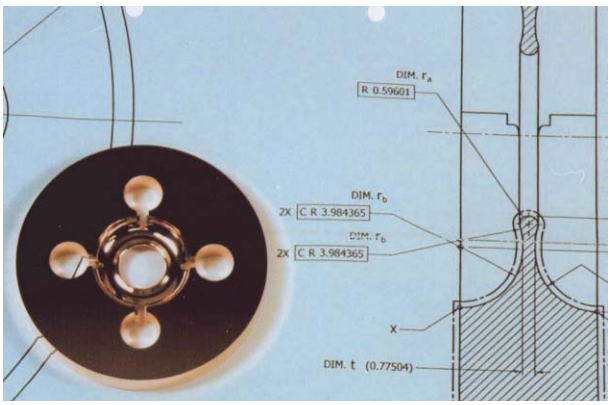

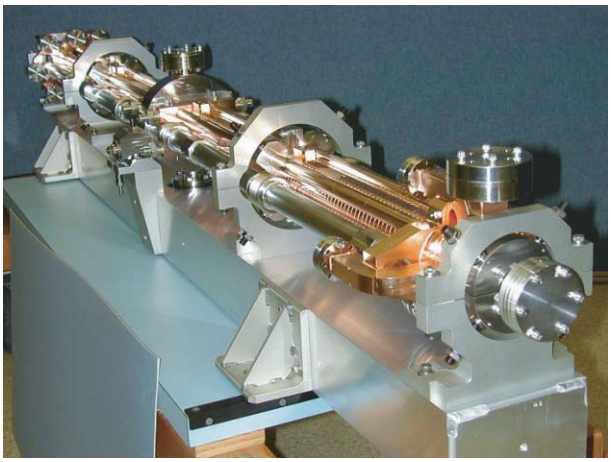

Figure 2: Unit cell anf full shape of an RDDS

at NLCTA of SLAC [5], but systematic measurements and analyses were focused on the following 8 structures [6]:

- 45 cm part ($v_g/c = 5\% \rightarrow 1.5\%$) of an already HiGT conditioned 1.8 m detuned structure with the input coupler renewed,
- 20 cm structure ($v_g/c = 5\% \rightarrow 4.4\%$) with diamond turned cells, 0.3μm cell etching before HiGT,
- 105 cm structure ($v_g/c = 5\% \rightarrow 1.5\%$) with diamond turned cells, 0.3μm cell etching,
- 1.8 m DDS ($v_g/c = 12\% \rightarrow 4.4\%$) with diamond turned cells and without cell etching,
- 53 cm structure ($v_g/c = 5\% \rightarrow 3.3\%$) with conventionally machined cells, 3μm cell etching,
- 53 cm structure ($v_g/c = 3.3\% \rightarrow 1.6\%$) with conventionally machined cells, 3μm cell etching,
- 53 cm structure ($v_g/c = 3.3\% \rightarrow 1.6\%$) with conventionally machined cells, 1.5μm cell etching, and a low-field/low-impedance input coupler,
- 53 cm structure ($v_g/c = 3.3\% \rightarrow 1.6\%$) with diamond turned cells and without cell etching.

At HiGT, the structures are processed at an RF pulse rate of 60 Hz with the pulses being progressively elongated to 240 ns (400 ns for the last two structures) for a target gradient. While the structures having the upstream v_g not greater than 5% were processed to 70 MV/m or over, the 1.8 m DDS was limited at around 50 MV/m, at which damage due to arc became serious. By a bead-pull method and measurements of beam-induced phases of the accelerating mode, phase errors of the accelerating mode were compared before and after HiGT. The 1.8 m DDS showed an accumulated phase change of $\sim 20^\circ$ after 1000 hours processing at under 50 MV/m. Furthermore, the change was mostly concentrated in the upstream half of the structure. On the other hand, the structures with $v_g = 5\%$ or less generally showed phase changes smaller than a few degrees after 1000 hours HiGT at over 70 MV/m. The HIGT history is shown in Fig 3.

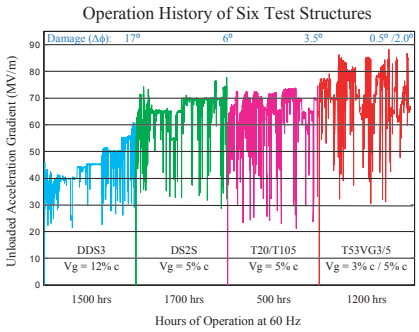

Figure 3: HiGT History at NLCTA [6]

In autopsy many pits on the order of 10μm or even completely melted surfaces due to HV breakdown were observed around the disk aperture. From bead-pull measurements, an order of magnitude larger volume was found missing for the 1.8 m DDS than the other structures. Those observations are consistent with a simple circuit analysis which shows the power absorbed at an arcing point is proportional to v_g^2 [5]. Considering those experimental results, a phase shift of 150° ($5\pi/6$ mode) is chosen in stead of the conventional $2\pi/3$ mode. This high-phase-advance structure type has the advantage of ensuring the same a/λ for a smaller v_g. Another way to solve the v_g problem is to choose a standing wave structures [10]. HiGT study is going on for 20 cm π mode structures in parallel with the TW structures. The breakdown rate seems to be at promising levels.

Further important observation with respect to the 53 cm structures is that breakdown rates at the structure body itself are from 0.2 to 0.3 per hour at levels from 70 to 73 MV/m, those at the input and output couplers are on the same order or sometimes an order of magnitude larger. In order to circumvent this problem, some new coupler designs are being considered, in which either field strengths or a local v_g are reduced. But SEM photos show a lot of arc pits are concentrated along the sharp ridges (curvature $\sim$ 80 μm) of the slot opening to the input waveguide [8][9]. According to calculations, surface magnetic fields along the ridges reach 0.7 MA/m, producing a pulsing temperature rise of about 130°C. The accompanied

stress may be an order of magnitude larger than copper's yield strength (54 MPa) and cause micro-fractures along the ridges. Hence another coupler design is in progress where the ridge curvature is made as large as a few mm. The same discussion should be applied for the HOM coupler slots of each cell. Therefore a similar rounding will be introduced for the latest cell design.

Clear conclusions have not yet been reached regarding surface treatments of cells before HiGT. Deep chemical etching seems to have some good effects for cells machined with a conventional lathe. Degassing in a hydrogen furnace seems to make the processing time much shorter according to DC HV breakdown tests of small Cu electrodes [7]. Those issues are to be investigated together with other ways of surface treatment.

For the NLC/JLC design, the breakdown rate along the full length of the main linacs should be within 1 per 10^6 pulses, which corresponds to 0.2 breakdowns per hour at 60 Hz operation. Present levels are still 2 to 3 times higher than this, although the rates in the structure body itself achieved the required level at 70 MV/m with 400 ns pulses. A phase change of 0.5° per 1000 hours operation at 120 Hz is required if the effective gradient decrease should be on the order of 5% in 20 years. The presently reached levels are within 2 times the requirement [6].

The near future plan for HiGT of TW structures will be as follows. A new high-phase-advance 90 cm structure is tested in the fall of 2002. Afterwards, test of two structures follows which have modified couplers. Except for a few of initial 1.8 m structures, all of the above structures have no HOM damping system. The first high-phase-advance DDS structure with the new HOM coupler design will be tested from the spring of 2003. There is a plan to set up a HiGT stand also at KEK in the summer of 2003.

5 RF POWER SOURCES

Details about X-band power sources are given by another talk in this conference [12]. A short summary is given below.

5.1 Klystron

As listed in Table 4, the NLC and JLC klystrons have the same design specifications for major parameters except for the pulse length which is 3.17μs for NLC, twice the JLC value.

Best results attained by NLC tubes are [13]: 70 MW peak RF power for 120 Hz, 300 ns pulses (efficiency = 55%) and 50 MW peak RF power for 120 Hz, 3.2μs pulses (efficiency = 39%) , while those for JLC tubes are: 68 MW peak RF power for 50 Hz, 1.5μs pulses (efficiency = 53%) . Second harmonic cavities are added in the latest JLC tube in order to improve the efficiency. Figure 4 shows a PPM klystron developed at KEK.

Of most concern is to suppress HOM oscillations. For the NLC tubes, while the penultimate cavity and the output cavity are made of copper, all the other RF cavities are made of stainless steel and every part of the beam tubes has stainless steel liner. The JLC tubes have the same configuration except that the penultimate cavity is also made of stainless steel. Furthermore, for the JLC tubes the two waveguides attached to the output cavity make an angle of not 180° but 150° in order to couple out the dangerous TE_{11} mode.

The permanent magnets are made of Nd-Fe-B tertiary alloy. They produce a peak axial field of over 3 kG between every two iron yokes placed at a pitch of 15 mm. Well aligned yokes and uniformly magnetized magnet pieces seem to be key points to get RF outputs of high quality.

Figure 4: X-band PPM Klystron developed at KEK

Table 4: Design Specifications of NLC/JLC Klystrons

Peak Power	75	MW
RF Pulse Length (NLC/JLC)	3.17 /1.59	μs
Rep. Rate (NLC/JLC)	120/150	Hz
Efficiency	55	%
Beam Voltage	506	kV
Beam Current	270	A
Perveance	0.75×10^{-6}	$\mathrm{AV}^{-3/2}$
Focusing	PPM	
Magnet Material	B-Nd-Fe	

5.2 DLDS

NLC and JLC have different DLDS designs owing to the different RF output pulse widths of the corresponding klystrons. For the NLC design, the 3.2μs pulses from one klystron station are sliced into four 400 ns, 100 MW sub-pulses, which are sequentially fed to four linac units placed $n \times 59.105$ m $(n = 0, 1, \ldots, 7)$ distant from the klystron station. Circular waveguides with a diameter of 120 cm are used for the long distance feed. In order to save the total length of the waveguides, each guide transports two 400 ns pulses, one in TE_{01} mode and the other in TE_{12} mode. Each tap-off point is equipped with a mode selector to choose a prescribed mode [11].

For the JLC design on the other hand, the 1.6μs pulses from one klystron station are divided into eight 400 ns, 100 MW sub-pulses, which are sequentially fed to eight linac units placed $n \times 58.806$ m $(n = 0, 1, 2, 3)$ distant from the klystron station. Only the TE_{01} mode is used for transmission and hence any mode selector is unnecessary. The longest distance is one half of the NLC case. Hence the waveguide has a smaller inner diameter of 90 mm. Although the waveguide density at a tunnel cross-section seems larger compared with the NLC case, JLC adopts a way of interleaving klystron stations, which makes the density profile much averaged to acceptable levels.

5.3 Modulator

Both NLC and JLC are developing modulators with IGBT (Insulated Gate Bipolar Transistor) solid-state switches which have less switching time jitters and longer life times than conventional thyratron switches. One induction unit comprises a toroidal core whose primary windings are driven by sets of IGBT switches and capacitors. Since the operation voltage of an IGBT induction unit is around 3 kV, many units are stacked together, the number of which depends on the number of turns of the secondary winding.

NLC adopts a 3-turn secondary. A prototype successfully drove four 5045 S-band klystrons in parallel by 1680 A, 380 kV, 3.2μs pulses at 120 Hz. The NLC design goal is to drive 8 NLC PPM klystrons listed in Table 4 [14].

The JLC modulator has a linear one-turn secondary. Therefore it is nothing but an induction linac of 550 kV. It is called linear induction modulator (LIM) [15]. The whole induction unit is 6 m long with the oil tank for socketing eight klystrons. Although it has a long shape, its width is less than 1.5 m and its height including the klystrons less than 2.5 m. Therefore JLC LIM's would not require any expansion of the tunnel cross-section, thus saving the tunnel cost. A prototype of JLC LIM is to be completed its fabrication in mid-2003.

6 CONCLUSIONS

R&D results at present have almost reached the design goals regarding such basic accelerator components as the X-band TW structures, klystrons, RF power distribution system, modulators, and low-emittance beam generation. Now we think it is a very urgent issue to complete in 2 years that one full fledged linac accelerator unit, which is at SLAC under construction as the 8-Pack Project and is at KEK being planned as the J-LUFT project.

7 REFERENCES

[1] H. Hayano, *Status of ATF*, report at LC2002 Linear Collider Work Shop (February 2002, SLAC). `http://lcdev.kek.jp/Conf/LC2002 /WG1_Hayano_H.pdf`

[2] Z. Li *et al.*, *Traveling Wave Structure Optimization for the NLC*, Proc. PAC2001(2001)3816.

[3] N. Toge ed., *International Study Group Report Progress Report*, KEK-Report 2000-7/SLAC R-59, April 2000.

[4] N. Toge, *JLC Progress*, contribution to LINAC2000, August 2000.

[5] C. Adolphsen *et al.*, *Processing Studies of X-band Accelerator Structures at the NLCTA*, Proc. PAC2001(2001)478.

[6] C. Adolphsen, *High Gradient R&D Results and Plans*, report at ISG8 meeting (June 2002, SLAC), `http://www.user.slac.stanford.edu/star/images /ISG8%206_02.pdf`.

[7] S. Kobayashi, *Effectiveness of Electrode Preparation Methods on the Characteristics of Pulsed DC High Voltage Conditioning*, report at LC2002 Linear Collider Work Shop (February 2002, SLAC). `http://lcdev.kek.jp/Conf/LC2002 /WG2_Kobayashi.pdf`

[8] V. Dolgashev, *Experiments on Gradient Liimits for Normal Conducting Accelerators*, this conference.

[9] F. Le Pimpec *et al.*, *Autopsy on an RF-Processed X-band Travelling Wave Structure*, LCC Notes **LCC-0097** (August 2002, SLAC) .

[10] R. Miller *et al.*, *Room Temperature Accelerator Structures for Linear Colliders*, Proc. PAC2001(2001)3819.

[11] C. Nantista, *NLC High Power RF Component Development*, report at ISG8 meeting (June 2002, SLAC), `http://www-project.slac.stanford.edu/lc/ilc /ISG_Meetings/ISG8/ISG8Comp-Nantista.pdf`.

[12] Y. Chin, *Worldwide Progress in X-Band Power Sources*, this conference.

[13] G. Caryotakis, *SLAC PPM Klystron Development*, report at ISG8 meeting (June 2002, SLAC), `http://www-project.slac.stanford.edu/lc/ilc /ISG_Meetings/ISG8/Caryotakis.pdf`.

[14] D. Schultz, *The 8-Pack Project*, report at ISG7 meeting (November 2001, KEK), `http://www-project.slac.stanford.edu/lc/local /Projects/8Pack/talks/ISG_Talk_11_01.pdf`.

[15] V. Vogel *et al.*, *Design of Linear Induction Modulator*, report at ISG8 meeting (June 2002, SLAC), `http://www-project.slac.stanford.edu/lc/ilc /ISG_Meetings/ISG8/Vogel_JLC_IGBT_mod.pdf`